New Journal of Physics
The open-access journal for physics

Surface plasmon polariton-mediated enhancement of the emission of dye molecules on metallic gratings

J Gómez Rivas[1], **G Vecchi and V Giannini**
FOM Institute for Atomic and Molecular Physics AMOLF,
c/o Philips Research Laboratories, High Tech Campus 4, 5656 AE, Eindhoven,
The Netherlands
E-mail: j.gomez@amolf.nl

New Journal of Physics **10** (2008) 105007 (14pp)
Received 22 May 2008
Published 28 October 2008
Online at http://www.njp.org/
doi:10.1088/1367-2630/10/10/105007

Abstract. We present measurements of iso-frequency dispersion surfaces of light scattered from metallic micro-gratings with different periods. The dispersion surfaces, obtained using an infinity-corrected microscope objective, exhibit maxima attributed to diffracted orders as they become evanescent and pronounced minima due to the resonant excitation of surface plasmon polaritons (SPPs). We have also measured the enhanced photoluminescence of a thin layer of dye molecules on top of the grating. This enhanced luminescence is attributed to the local field enhancement close to the surface due to the coupling of the excitation frequency to SPPs. Moreover, we obtain a directional emission of the luminescence, which is attributed to the grating-assisted coupling of SPPs excited by the dye to free space light. The technique used for the measurements presented in this paper can be extended to characterize the angular emission patterns of emitters coupled to micro- and nano-plasmonic structures.

[1] Author to whom any correspondence should be addressed.

Contents

1. Introduction

Surface polaritons are electromagnetic waves coupled to a polarization charge at the interface between two media with different permittivities [1]. If these media are a metal and a dielectric the polarization charge arises from the collective oscillation of the free electrons in the metal and the surface polaritons are called surface plasmon polaritons (SPPs) [2]. Several promising applications are driving the renewed interest in surface plasmon optics or plasmonics. The evanescent character of SPPs, with long propagation lengths of several wavelengths along the surface and evanescent decay of the field away from the interface, has led to an increased interest in plasmonics for data transmission in optical interconnects [3]. The large local-field enhancement close to the interface and the resonant condition for the excitation of SPPs are used for the sensitive detection of analytes bound to metallic surfaces [4]. The possibility of modifying the emission characteristics of light from emitters close to metallic structures has triggered intensive research toward the improvement of the efficiency of LEDs and OLEDs [5]–[9].

The evanescent character of SPPs leads to a momentum or wavenumber parallel to the surface larger than the wavenumber of free space electromagnetic radiation. Therefore, it is not possible to excite SPPs by illuminating a flat metallic surface. SPPs can be generated by the diffracted orders of light scattered from a metallic grating [2]. This scattered radiation has a larger momentum than that of the incident radiation by an integer number of reciprocal lattice vectors. Grating-assisted coupling to SPPs was already observed by Wood in 1902 when he reported dips in the specular reflection of metallic gratings [10].

Grating-assisted excitation of SPPs is usually investigated by illuminating a grating with a collimated beam of light and detecting dips in the specular reflection [11]. However, this is a cumbersome technique as it requires relatively large gratings and several measurements at different angles of incidence. In this paper, we use an infinity-corrected microscope objective to image the scattered light from micro-gratings in reciprocal space. In this way, we are able to measure iso-frequency dispersion surfaces with a single measurement. Similar techniques have been used previously to measure the dispersion of SPPs on metallic gratings [12]–[15]. In particular, we observe an increase of the reflected intensity relative to the reflection of a flat surface at positions in reciprocal space at which the diffracted orders become evanescent, i.e. the so-called Rayleigh anomalies [16]. We also observe Wood anomalies, or a decrease of

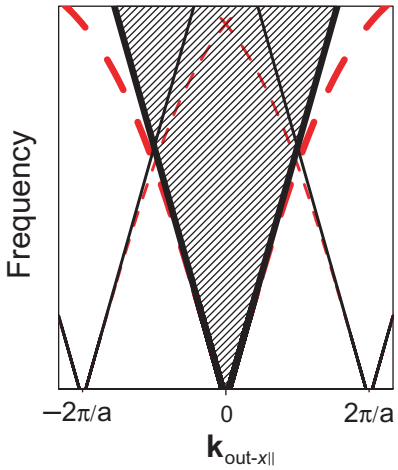

Figure 1. Dispersion relation of light scattered by a grating (black solid lines) and of SPPs on a periodically corrugated metallic surface (red-dashed curves). The shaded area represents the light cone.

the reflection at positions of larger momentum than the Rayleigh anomalies, corresponding to the resonant excitation of SPPs.

By spinning a thin layer of dye molecules onto a grating and measuring their photoluminescence, we also demonstrate an enhanced and directional emission. This enhanced and directional luminescence originates from the local field enhancement of the laser light used to optically pump the dye and the grating-assisted coupling of SPPs excited by the dye to free space radiation. SPP directional enhancement of the luminescence of fluorophores by gratings has been reported in the past [17]–[21]. The technique commonly used in these studies involves the scanning of the angle of incidence of the excitation beam onto the grating and/or the angle of detection of the photoluminescence. This is in contrast to our measurements in which the sample is illuminated by a range of k-vectors and a solid angle is detected by means of an infinity-corrected microscope objective.

2. Iso-frequency dispersion surfaces

The iso-frequency dispersion surface measurements presented in the next section can be easily understood by first having a look at the dispersion relation of light scattered from a grating. Light is scattered according to the relation

$$\mathbf{k}_{\text{out}\parallel}(\omega) = \mathbf{k}_{\text{in}\parallel}(\omega) \pm m\mathbf{G}, \tag{1}$$

where $\mathbf{k}_{\text{in}\parallel}$ and $\mathbf{k}_{\text{out}\parallel}$ are the incident and scattered wave vectors parallel to the surface of the grating, i.e. $\mathbf{k}_{\text{in}\parallel} = (\omega/c)\sin\theta_{\text{in}}$ and $\mathbf{k}_{\text{out}\parallel} = (\omega/c)\sin\theta_{\text{out}}$, θ_{in} and θ_{out} being the angles measured with respect to the surface normal, ω the angular frequency and c the speed of light in the dielectric on top of the grating. $\mathbf{G}$ is the reciprocal lattice vector of the grating, of modulus $2\pi/a$ and that we consider in this paper along the x-direction, where a is the period of the grating and m is an integer.

The dispersion relation of light scattered from the grating when the incident k-vector is in the plane containing the reciprocal lattice vector and the surface normal (x–z-plane) is schematically represented in figure 1. In this figure, the thick black lines correspond to

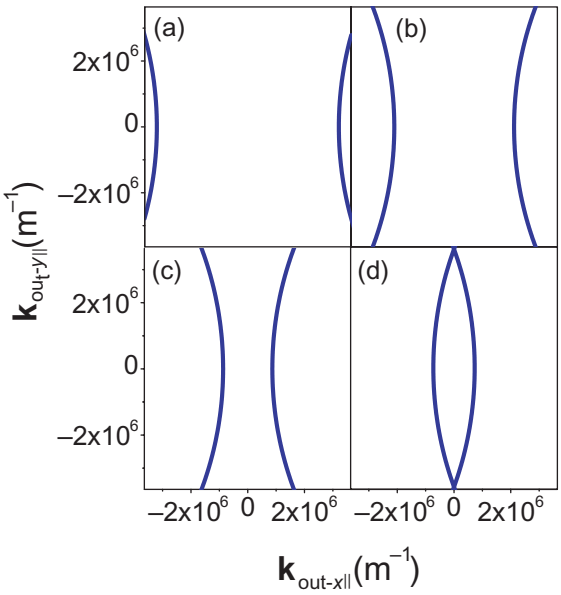

Figure 2. Dispersion surfaces of the Rayleigh anomalies of gratings with period (a) 510, (b) 580, (c) 630 and (d) 750 nm, calculated at a wavelength $\lambda = 690$ nm.

$\mathbf{k}_{\text{out-}x\parallel} = \omega/c$, i.e. the $m = 0$ order for $\theta_{\text{in}} = \theta_{\text{out}} = 90^\circ$. The shaded area in figure 1 represents the light cone and it contains all the modes accessible by light scattered from the grating. The thin black lines are the $m = \pm 1$ diffracted orders of maximum momentum. These thin black lines define the Rayleigh anomalies or the wavenumbers of the diffracted orders at the frequencies at which these orders become evanescent [22].

Figure 2 displays a calculation of the iso-frequency dispersion surface, i.e. the surface in the dispersion relation at a constant frequency, of the $m = \pm 1$ Rayleigh anomalies. For a later comparison with measurements, figure 2 was obtained by considering a wavelength $\lambda = 690$ nm, grating periods of 510 nm (a), 580 nm (b), 630 nm (c) and 750 nm (d), and wavenumbers of the scattered light parallel to the surface, $\mathbf{k}_{\text{out-}x\parallel}$ and $\mathbf{k}_{\text{out-}y\parallel}$, in a range limited by a numerical aperture NA $= 0.4$, i.e. smaller than $(2\pi/\lambda)$NA.

The red thick dashed curves in figure 1 represent the dispersion relation of SPPs on a metallic grating. In the limit of shallow gratings, this dispersion relation can be approximated to

$$\mathbf{k}_{\text{SPP}}(\omega) \simeq (\omega/c)\text{Re}\left\{[\epsilon_{\text{m}}(\omega)\epsilon_{\text{d}}(\omega)/(\epsilon_{\text{m}}(\omega)+\epsilon_{\text{d}}(\omega))]^{1/2}\right\}, \tag{2}$$

where $\mathbf{k}_{\text{SPP}}$ is the wave vector of SPPs parallel to the surface, ϵ_{m} is the permittivity of the metal, with $\text{Re}(\epsilon_{\text{m}}) < -1$, and $\epsilon_{\text{d}} > 1$ the permittivity of the dielectric. Due to the evanescent character of SPPs, $\mathbf{k}_{\text{SPP}}$ is always larger than ω/c, i.e. the dispersion relation of SPPs is outside the light cone. Therefore, coupling between free space electromagnetic waves and SPPs has to be mediated by the $m = \pm 1, \pm 2, \ldots$ scattered orders from the grating. This coupling takes place when the phase matching condition

$$\mathbf{k}_{\text{in}_\parallel} \pm m\mathbf{G} = \pm\mathbf{k}_{\text{SPP}} \tag{3}$$

is satisfied, namely when the dispersion relation of the scattered SPPs (thin red dashed curves in figure 1) lies within the light cone.

SPPs can also be excited by near-field coupling of light emitters close to metals. If an emitter is located in the proximity of a metallic surface it can decay non-radiatively by coupling

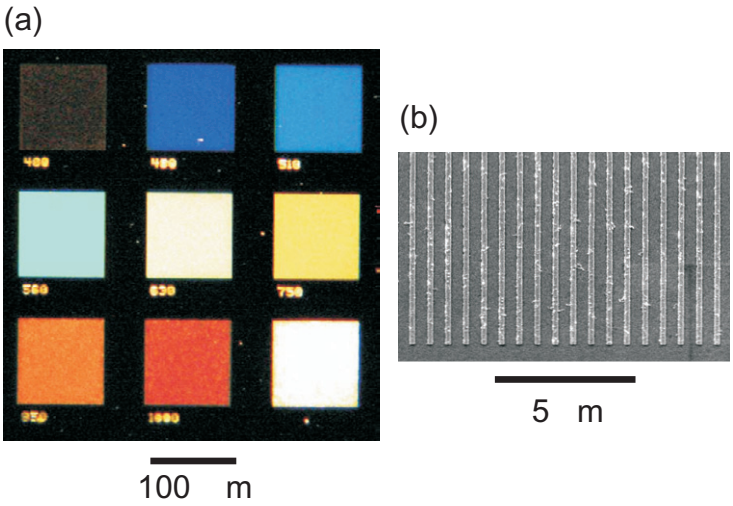

Figure 3. (a) Dark-field optical microscope image of Au gratings with a period varying from 400 (up-left grating) to 1000 nm (bottom-middle grating). (b) Scanning electron microscope image of an Au grating with a period of 630 nm, a ridge height of 40 nm and a ridge width of 200 nm.

to SPPs. This near-field coupling causes the quenching of the photoluminescence [23, 24]. By patterning a metallic surface with a grating it is possible to couple these SPPs back to free space light with a wave vector given by the relation

$$\mathbf{k}_{\mathrm{out}_{\parallel}} = \pm\mathbf{k}_{\mathrm{SPP}} \pm m\mathbf{G}. \tag{4}$$

This phenomenon leads to the grating-assisted directional emission from emitters in the proximity of metals [17, 18].

3. Sample fabrication and experimental setups

3.1. Metallic gratings

A set of eight gold micro-gratings with a size of $100 \times 100\,\mu$m and with varying periods from 400 up to 1000 nm were fabricated using standard e-beam lithography and lift-off. The fabrication is as follows: a layer of Au with a thickness of 300 nm was sputtered on top of a Si wafer. This layer is optically thick and can be considered as semi-infinite. Gratings were defined by an electron beam on a layer of photo-resist spincoated on top of the Au surface. A layer of Au with a thickness of 40 nm was evaporated after having etched the exposed regions of the photo-resist with the electron beam. This additional layer of Au demarcated the ridges of the gratings once the remaining photo-resist was removed by a liftoff process. The gratings investigated in this paper had ridges with a width of 200 nm and periods of 510, 580, 630 and 750 nm. Due to the small dimensions of the gratings, the scattering of light was studied using an infinity-corrected microscope objective to obtain the iso-frequency dispersion surfaces.

Figure 3(a) shows an optical microscope image of the micro-gratings with varying lattice constants. This photograph was taken using a low-numerical aperture dark-field objective ($\times 10$, NA $= 0.25$). The colors in this image arise from the diffraction of light on gratings with

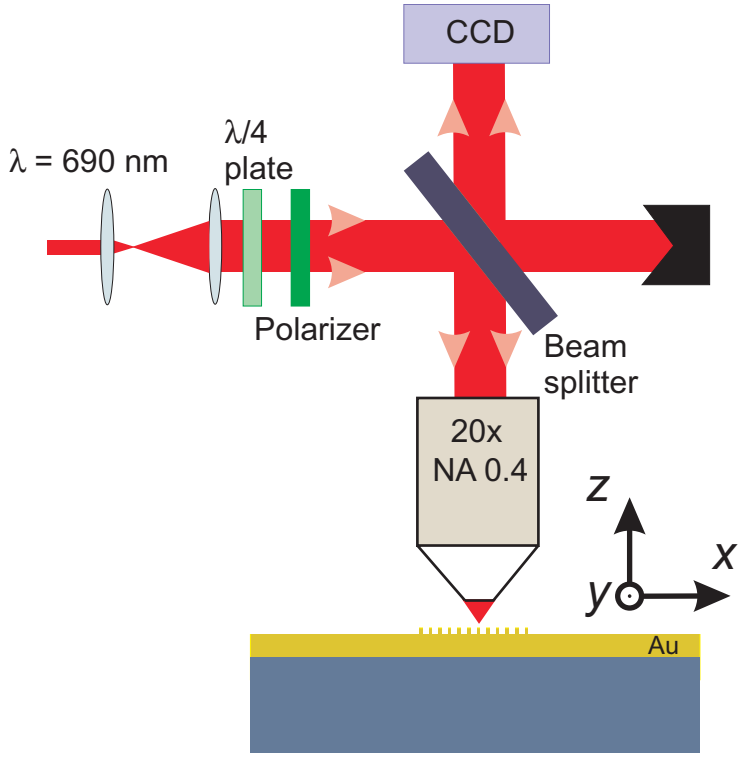

Figure 4. Schematic representation of the optical setup used to obtain the iso-frequency dispersion surfaces of Au gratings. The expanded beam of a laser diode ($\lambda = 690$ nm) is focused onto the sample by a microscope objective. The scattered light is collected by the same objective and imaged by a CCD camera. The system of coordinates used throughout this paper is also displayed.

different periods. A scanning electron microscope image of the grating with a period of 630 nm is shown in figure 3(b).

We prepared a similar grating to measure the SPP-assisted enhancement of the luminescence of dye molecules. This grating had a period of 630 nm, ridges with a height of 30 nm and a width of 200 nm. On top of the grating, we spun a layer with a thickness of 40 nm of dye molecules (Atto 680, Atto-Tech GmbH) embedded in a polymer (polyvinyl butyral, PVB) matrix. The large dimensions of this grating (3×3 mm^2) allowed us to measure the photoluminescence in two different manners: with the aforementioned infinite-corrected microscope and by illuminating the grating with a collimated beam and varying the angle of incidence.

3.2. Experimental setups

The iso-frequency dispersion surfaces were measured with the setup represented schematically in figure 4. The beam from a laser diode ($\lambda = 690$ nm) was expanded and its polarization state was set to p-polarized by means of a $\lambda/4$ plate and a polarizer. This expanded beam was sent through a beam splitter into a bright-field infinity-corrected microscope objective ($\times 20$, NA $= 0.4$). In this way, the laser beam was focused onto the surface of the gratings.

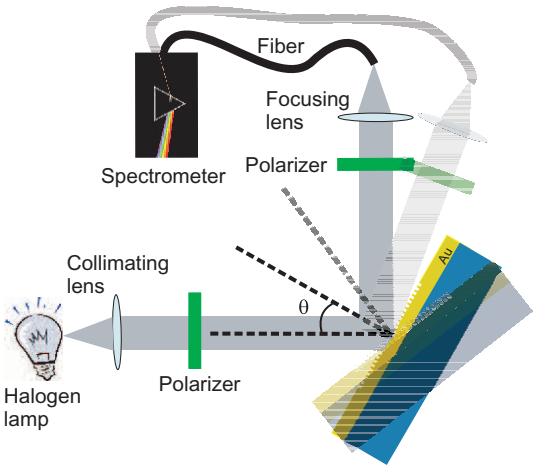

Figure 5. Schematic representation of the setup used to measure the specular reflection of Au gratings. A collimated beam from a halogen lamp is reflected by the grating and detected with a fiber-coupled spectrometer. The grating and detector can rotate to vary the angle of incidence and detection. Photoluminescence measurements of dye molecules on the grating were done by using a laser to excite the molecules and detecting the photoluminescence with a photodiode at a fixed direction and for different angles of incidence, after filtering out the laser light (laser, filter and photodiode not shown in the figure).

The reflected light was collected by the same objective. The back focal plane of the microscope objective was imaged by an electron multiplying CCD camera (Luca DL-658M, Andor Technology). This back focal plane image represents a projection of the Fourier space on the plane of the CCD camera. The camera was placed parallel to the surface of the grating and, according to equation (1), each pixel in the images corresponds to a scattered wave vector parallel to the surface of the grating. The smallest $\mathbf{k}_{\text{out-}x\parallel}$ and $\mathbf{k}_{\text{out-}y\parallel}$ are 0 and correspond to the central pixel of the images, whereas the largest detected $\mathbf{k}_{\text{out-}x\parallel}$ and $\mathbf{k}_{\text{out-}y\parallel}$ are determined by the maximum collection angle of the microscope objective, i.e. the NA of the objective. Photoluminescence measurements were also done with this setup by placing a band-pass filter in front of the electron multiplying CCD camera (not shown in figure 4) with a central wavelength of 750 nm, i.e. at the emission of the dye (Atto 680, Atto-Tech GmbH), a transmission bandwidth of 40 nm, and an out-of-band transmission smaller than 0.01%. The maximum absorption cross section of the dye is at a wavelength of 680 nm, i.e. very close to the wavelength of the laser diode used in the experiments.

Specular reflection and photoluminescence measurements were done on the $3 \times 3\,\text{mm}^2$ gratings by illuminating them with a collimated beam and rotating the grating and detector. A schematic representation of the setup is displayed in figure 5. For the reflection measurements, we used a halogen lamp and the reflected beam was sent to an optical fiber connected to a spectrometer. Sample and fiber were mounted onto computer-controlled rotation stages, which allowed to scan the angle of incidence onto the sample and detect the specular reflection. The photoluminescence measurements on the large area grating were done by illuminating the grating covered with dye with a collimated beam from the $\lambda = 690\,\text{nm}$ laser diode. The photoluminescence was detected by a silicon photodiode. Any residual pump light was blocked

by a 750 ± 20 nm band-pass filter placed in front of the detector. The sample was rotated with respect to the direction of the incident beam, whereas the detector was rotated keeping always a fixed angle of 3° with respect to the normal of the grating.

In the next section, we describe iso-frequency dispersion measurements in micro-gratings and specular reflection spectra of large gratings. These measurements reveal the grating-assisted excitation of SPPs. As a consequence of this resonant excitation of SPPs, we obtain an enhancement of the photoluminescence of dye molecules close to the surface.

4. Iso-frequency dispersion surfaces and angular-resolved measurements

4.1. Reflection measurements

Figure 6 displays the iso-frequency dispersion surfaces measured at $\lambda = 690$ nm of the scattered light from Au micro-gratings with different periods. To obtain the relative reflection and correct for aberrations in the optical system, each measurement on a grating was normalized by the reflection on a flat Au surface. The images correspond to the scattered light from the gratings of periods (a) 510, (b) 580, (c) 630 and (d) 750 nm. We have also plotted in figure 6(e) the normalized intensity along the dotted lines of figures 6(a) and (d). The bands of increased intensity correspond to the $m = \pm 1$ Rayleigh anomalies and are in good agreement with the calculations in figure 2. When a diffracted order becomes evanescent more intensity is available to other orders and the reflectance of the grating increases. The bands of reduced intensity in figure 6 correspond to the resonant coupling to SPPs by scattering of the incident beam from the metallic grating. Coupling the incident light into a electromagnetic surface mode is accompanied by a reduction of the reflected intensity. In the next section, we demonstrate that this resonant coupling to SPPs leads to an enhancement of the pump intensity of fluorophores on top of the grating.

The specular reflection spectra of p-polarized light on the large area (3×3 mm^2) gratings are presented in figure 7 as functions of the angle of incidence. These spectra have been normalized by the reflection spectra of an Au mirror. Figure 7(a) corresponds to the reflection of an Au grating, whereas 7(b) is the reflection of a similar grating covered by a PVB layer with a thickness of 40 nm containing dye molecules. The bands of reduced specular reflection correspond to the resonant excitation of SPPs. The thin polymer layer with $\epsilon_d = 2.2$ on top of the grating produces a shift of the SPPs resonances. Figure 7(c) displays the normalized specular reflection spectra for an angle of incidence of 6° of the grating without PVB layer (red squares) and with PVB layer (blue circles). Note that the Rayleigh anomalies are not visible in these measurements, in contrast to the measurements of the iso-frequency dispersion surfaces. This difference is probably due to the smaller height of the ridges in the large area gratings, which leads to a smaller separation of the Wood and Rayleigh anomalies and their overlapping within our experimental resolution.

4.2. Photoluminescence measurements

The electromagnetic local field is enhanced at the surface of a grating when the incident radiation is resonantly coupled to SPPs. This enhancement is illustrated in figure 8, where the intensity of the magnetic field component along the y-direction (the direction parallel to the ridges of the grating), normalized by the incident intensity, is represented for a p-polarized plane

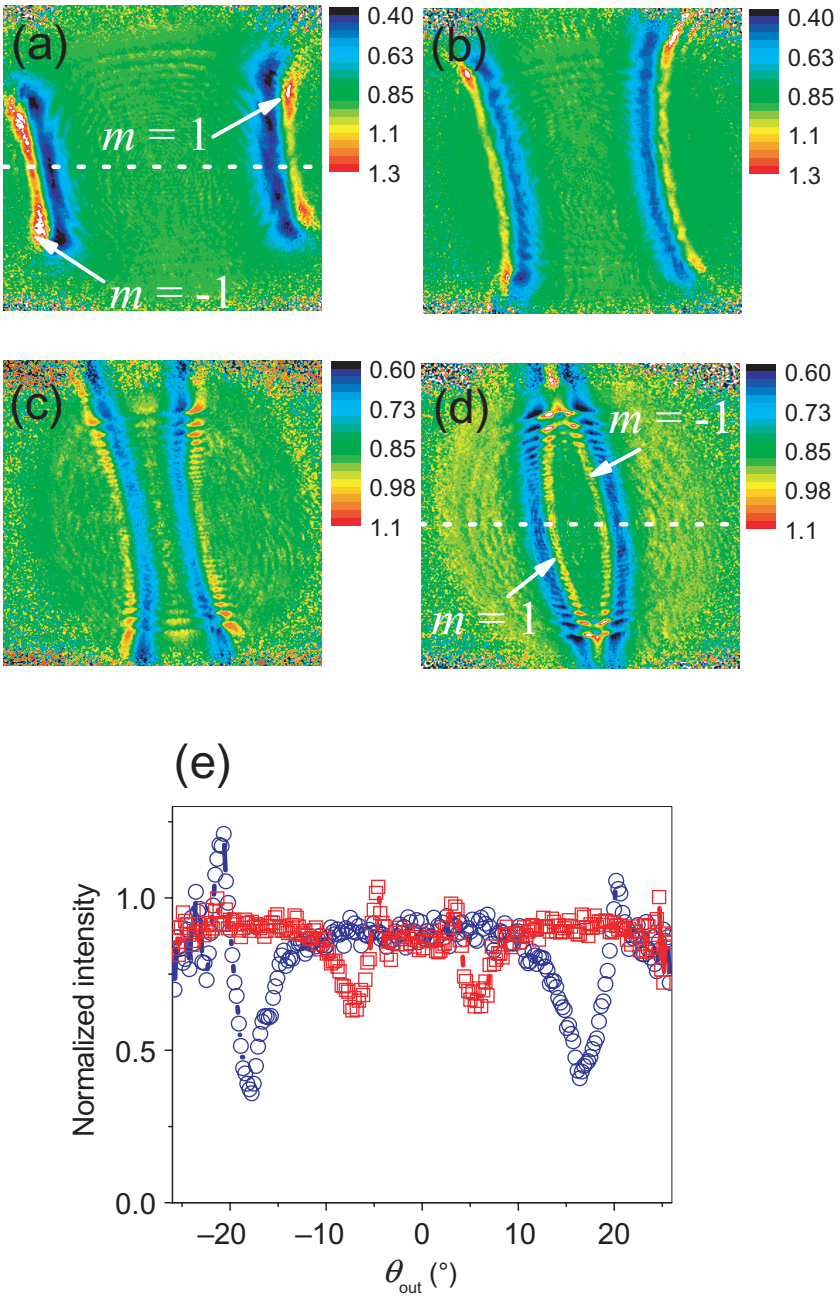

Figure 6. Iso-frequency dispersion surfaces of the scattered intensity at $\lambda = 690$ nm from Au gratings with periods (a) 510, (b) 580, (c) 630 and (d) 750 nm, normalized by the intensity reflected on a flat Au surface. The $m = \pm 1$ Rayleigh anomalies are indicated in (a) and (d). The open circles and squares in (e) correspond to this normalized intensity along the dotted lines of (a) and (d), respectively.

wave ($\lambda = 690$ nm) incident on an Au grating with a period of 630 nm. We have considered a permittivity of 2.2 for the dielectric on top of the grating. This calculation was done using the rigorous scattering equations of Green's theorem surface integral [25]. Figure 8(a) corresponds

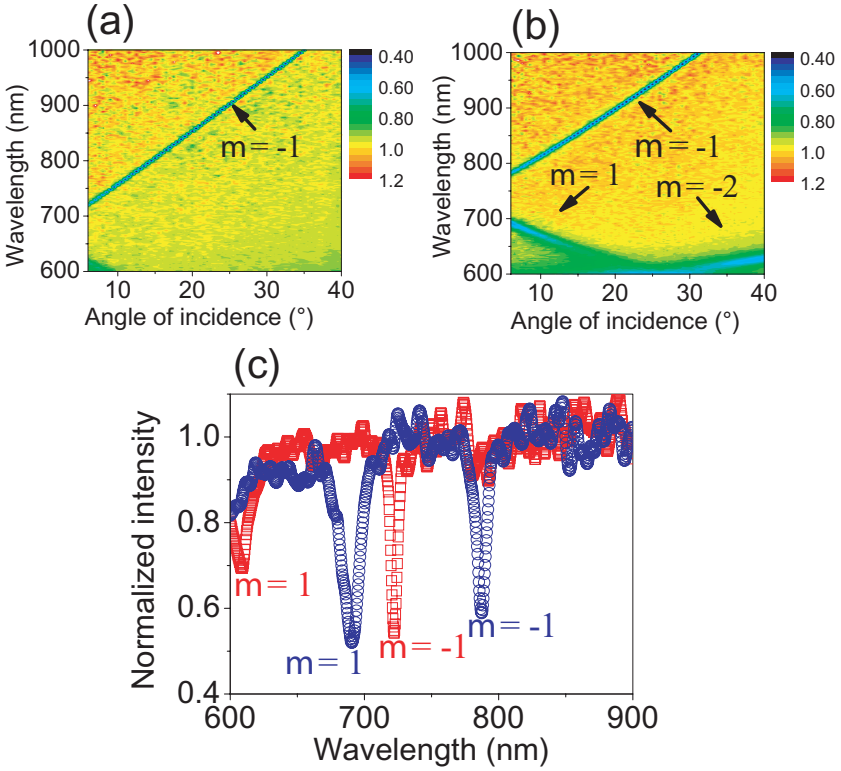

Figure 7. Specular reflection spectra of an Au grating normalized by the reflection on an Au mirror. (a) corresponds to the reflection on a grating with a period of 630 nm, ridges with a width of 200 nm and a height of 30 nm. The measurements in (b) correspond to a similar grating covered by a layer of dye molecules in a PVB matrix. This layer has a thickness of 40 nm. In (c) are displayed the normalized spectra measured at an angle of incidence of 6° for the grating without PVB layer (red squares) and with PVB layer (blue circles). The different orders of excitation of SPPs have been labeled in the figures.

to normal incidence ($\theta_{in} = 0°$), i.e. for a non-resonant angle of incidence. The calculation of figure 8(b) corresponds to ($\theta_{in} = 21°$), i.e. the angle of excitation of SPPs by the $m = -1$ diffracted order. The incident intensity can be enhanced up to 40 times at certain locations on the surface due to the excitation of SPPs. The average enhancement at a distance of 40 nm from the surface (equal to the thickness of the dye layer) is 8.3 times the incident intensity.

The near-field enhancement for certain angles of incidence, i.e. for certain k-vectors, should lead to an enhanced excitation of light emitters placed onto the grating. We have demonstrated this pump enhancement by measuring the photoluminescence of the dye when the sample is illuminated with a collimated beam (beam diameter $\simeq$2 mm). These measurements are presented in figure 9 as a function of the angle of incidence. The angle formed by the incident k-vector parallel to the surface and the reciprocal lattice vector was kept constant at 0°. The open circles in this figure correspond to normalized photoluminescence measured when the excitation laser beam was p-polarized. The angle of maximum photoluminescence at 6° is consistent with the reduction of the specular reflection due to the coupling to SPPs through the $m = 1$ order (blue circles in figure 7(c)). The difference in the angle of resonant coupling

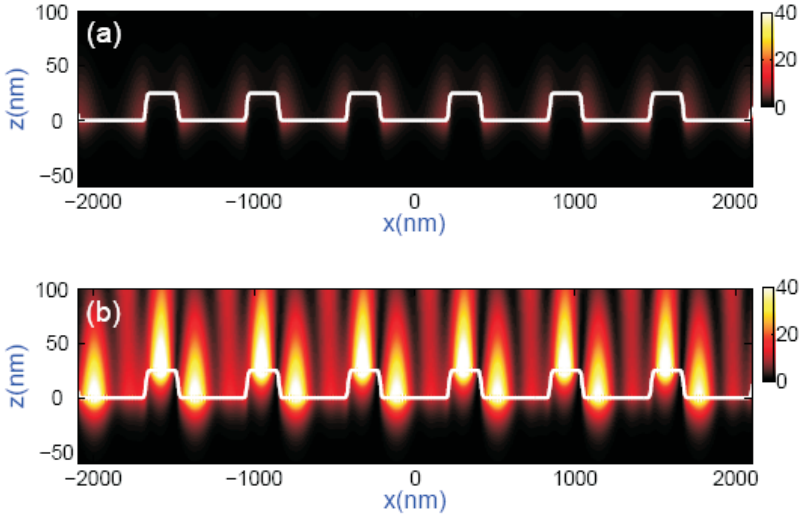

Figure 8. Near-field intensity for $\lambda = 690$ nm of the magnetic field component along the y-direction normalized by the incident intensity of p-polarized light incident on an Au grating. The grating has a period of 630 nm, height of the ridges of 30 nm and width of the ridges of 200 nm. The medium on top of the grating has a permittivity of 2.2. (a) corresponds to an angle of incidence of 0°, whereas the calculation in (b) is for an angle of incidence of 21°.

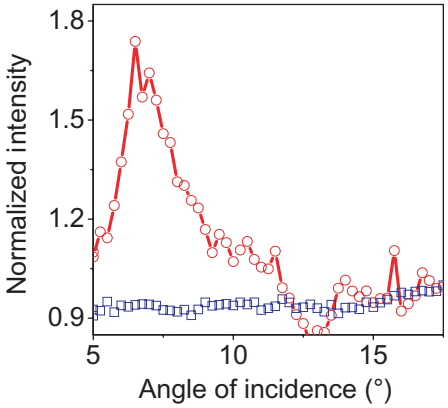

Figure 9. Photoluminescence intensity of dye molecules on top of an Au grating with period 630 nm normalized by the photoluminescence intensity of a layer of dye on top of a flat Au surface measured as a function of the angle of incidence of the excitation beam. The red circles correspond to p-polarized excitation, whereas the blue squares represent the photoluminescence for s-polarized excitation.

to SPPs between experiments and calculations is due to the finite thickness of the polymer layer in the experiment in contrast to the semi-infinite medium considered for the calculations. The blue squares in figure 9 correspond to the normalized photoluminescence measured for an s-polarized excitation. For this polarization, the incident beam does not couple to SPPs and the photoluminescence is not enhanced.

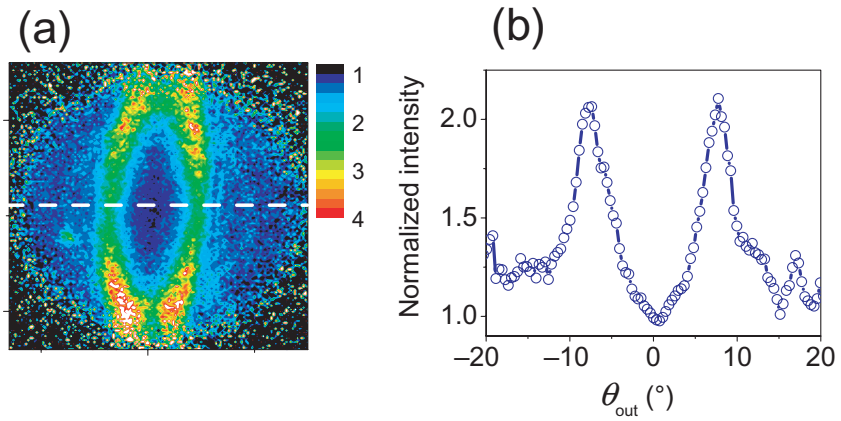

Figure 10. (a) Iso-frequency dispersion surface of the photoluminescence of the dye on top of a grating measured at a wavelength of 750 ± 20 nm. The image is normalized by the photoluminescence of a layer of dye on top of a flat Au surface. The data in (b) correspond to the photoluminescence intensity along the dashed line in (a).

Although the calculations in figure 8 were performed to illustrate the phenomenon of pump enhancement rather than to fit the measurements, it is interesting to point out some possible factors causing the smaller measured enhancement of the photoluminescence in figure 9: the calculation is performed for two semi-infinite media, while in the experiments the dye is embedded in a thin polymer layer in between air and the metal. Moreover, in the calculation we have not considered the absorption of the excitation light by the dye, which leads to a reduction of the field enhancement [20]. Also, within the assumption that the dye molecules are randomly oriented, only those having a dipole moment parallel to the local electric field will contribute to the emission. Another possible cause of reduction of the enhancement can be attributed to photo-bleaching and saturation of the dye at the positions of maximum pump field enhancement [20]. A quantitative evaluation of all these effects is beyond the scope of this paper.

We have also measured the iso-frequency dispersion surface of the photoluminescence emitted by the dye at $\lambda = 750 \pm 20$ nm using the infinity-corrected microscope objective. The laser light of $\lambda = 690$ nm, which excited the dye, was sent through the objective, therefore illuminating the grating in a range of angles determined by the numerical aperture. With this configuration, the dye on the grating is pumped by light incident at angles which are both resonant and non-resonant with the excitation of SPPs. The photo-excited dye decays emitting light or couples to the metal, exciting SPPs. These SPPs can be coupled by the grating into free space light at certain angles given by equation (4). The measurement of the photoluminescence, normalized by the intensity emitted by a layer of dye on top of a flat Au surface, is displayed in figure 10(a), where two emission bands are clearly visible. The plot in figure 10(b) represents the photoluminescence intensity along the dashed line in figure 10(a). The maxima of the dye emission (at $\pm 7.5^\circ$ for 750 nm) are slightly shifted with respect to the minimum in reflection of figure 7(b) (780 nm at 7.5°). The reason for this shift is unclear, although it may be partially explained by the local heating of the sample with the focused laser beam, which can lead to a small change in the refractive index of the polymer and a shift of the resonances [26].

An interesting extension of the technique used here to measure the photoluminescence of dye on a metallic grating could be the characterization of the enhanced spatial coherence and directionality in the emission of light sources coupled to metallic nanostructures such as nanoantennas [27]–[29].

5. Summary

Using an infinity-corrected microscope objective, we have investigated the scattering of light from Au micro-gratings with different periods. In particular, we have measured the iso-frequency dispersion surfaces at $\lambda = 690\,\text{nm}$. These surfaces exhibit maxima attributed to diffracted orders as they become evanescent and minima due to the coupling to SPPs. The electromagnetic field enhancement at the surface of the grating due to the coupling of the incident light to SPPs leads to a pump enhancement of light emitters. We have demonstrated this pump enhancement by measuring an increase of the photoluminescence intensity of dye molecules on top of an Au grating at angles of incidence resonant with the excitation of SPPs. We have also measured directional photoluminescence of the dye molecules using an infinity-corrected objective. This directionality is attributed to the non-radiative decay of the excited dye to SPPs modes and the coupling of these modes by the grating into free space radiation. The technique presented here can be extended to measure the directionality of light sources coupled to metallic nanostructures.

Acknowledgments

We acknowledge B Ketelaars for the fabrication of the gratings, M M M Vervest, H W M de Barse and H A G Nulens for SEM and AFM measurements, Y Zhang for preparing the dye-coated grating, and J A Sánchez-Gil and A F Koenderink for stimulating discussions. This work is part of the research program of the Stichting voor Fundamenteel Onderzoek der Materie (FOM), which is financially supported by the Nederlandse Organisatie voor Wetenschappelijk Onderzoek (NWO), and is part of an industrial partnership program between Philips and FOM.

References

[1] Agranovich V M and Mills D L (ed) 1982 *Surface Polaritons: Electromagnetic Waves at Surfaces and Interfaces* (Amsterdam: North Holland)
[2] Raether H 1988 *Surface Plasmons on Smooth and Rough Surfaces* (Berlin: Springer)
[3] Barnes W L, Dereux A and Ebbesen T W 2003 Surface plasmons subwavelength optics *Nature* **424** 824–30
[4] Homola J (ed) 2006 *Surface Plasmons Resonance Based Sensors* (Berlin: Springer)
[5] Gifford D K and Hall D G 2004 Emission through one of two metal electrodes of an organic light-emitting diode via surface-plasmon cross coupling *Appl. Phys. Lett.* **81** 4315–7
[6] Wedge S, Wasey J A E, Barnes W L and Sage I 2004 Coupled surface plasmon-polariton mediated photoluminescence from a top-emitting organic light-emitting structure *Appl. Phys. Lett.* **85** 182–4
[7] Okamoto K, Niki I, Scherer A, Narukawa Y, Mukai T and Kawakami Y 2005 Surface plasmon enhanced spontaneous emission rate of InGaN/GaN quantum wells probed by time-resolved photoluminescence spectroscopy *Appl. Phys. Lett.* **87** 071102
[8] Liu C, Kamaev V and Vardenya Z V 2005 Efficiency enhancement of an organic light-emitting diode with a cathode forming two-dimensional periodic hole array *Appl. Phys. Lett.* **86** 143501

[9] Tutt L and Revelli J F 2008 Distribution of radiation from organic light-emitting diode structures with wavelength-scale gratings as a function of azimuth and polar angles *Opt. Lett.* **33** 503–5
[10] Wood R W 1902 On a remarkable case of uneven distribution of light in a diffraction grating spectrum *Phil. Mag.* **4** 396–402
[11] Hibbins A P, Sambles J R and Lawrence C R 1998 Azimuth-angle-dependent reflectivity data from metallic gratings *J. Mod. Opt.* **45** 1019–28
[12] Swalen J D, Gordon J G, Philpott M R, Brillante A, Pockrand I and Santo R 1980 Plasmon surface polariton dispersion by direct optical observation *Am. J. Phys.* **48** 669–72
[13] Kitson S C, Barnes W L, Bradberry G W and Sambles J R 1996 Surface profile dependence of surface plasmon band gaps on metallic gratings *J. Appl. Phys.* **79** 7383–5
[14] Giannattasio A and Barnes W L 2005 Direct observation of surface plasmon-polariton dispersion *Opt. Express* **13** 428–34
[15] Ujué-González M, Stepanov A L, Weeber J-C, Hohenau A, Dereux A, Quidant R and Krenn J R 2007 Analysis of the angular acceptance of surface plasmon Bragg mirrors *Opt. Lett.* **32** 2704–6
[16] Rayleigh L 1907 Note on the remarkable case of diffraction spectra described by Prof. Wood *Phil. Mag.* **14** 60–5
[17] Knoll W, Phipott M R, Swalen J D and Girlando A 1981 Emission of light from Ag metal gratings coated with dye monolayer assemblies *J. Chem. Phys.* **75** 4795–9
[18] Gruhlke R W, Holland W R and Hall D G 1986 Surface-plasmon coupling in molecular fluorescence near a corrugated thin metal film *Phys. Rev. Lett.* **56** 2838–41
[19] Knobloch H, Brunner H, Leitner A, Aussenegg F and Knoll W 1993 Probing the evanescent field of propagating plasmon surface polaritons by fluorescence and Raman spectroscopies *J. Chem. Phys.* **98** 10093–5
[20] Kitson S C, Barnes W L, Sambles J R and Cotter N P K 1996 Excitation of molecular fluorescence via surface plasmon polaritons *J. Mod. Opt.* **43** 573–82
[21] Hung Y-J, Smolyaninov I I, Davis C C and Wu H-C 2006 Fluorescence enhancement by surface gratings *Opt. Express* **14** 10825–30
[22] Wood R W 1935 Anomalous diffraction gratings *Phys. Rev.* **48** 928–37
[23] Ford G W and Weber W H 1984 Electromagnetic interaction of molecules with metal surfaces *Phys. Rep.* **113** 195–287
[24] Barnes W L 1998 Fluorescence near interfaces: the role of photonic mode density *J. Mod. Opt.* **45** 661–99
[25] Giannini V and Sànchez-Gil J A 2007 Calculations of light scattering from isolated and interacting metallic nanowires of arbitrary cross section by means of Green's theorem surface integral equations in parametric form *J. Opt. Soc. Am.* A **24** 2822–30
[26] Nikolajsen T, Leosson K and Bozhevolnyi S I 2004 Surface plasmon polariton based modulators and switches operating at telecom wavelengths *Appl. Phys. Lett.* **85** 5833–5
[27] Gersen H, Garcia-Parajó M F, Novotny L, Veerman J A, Kuipers L and van Hulst N F 2000 Influencing the angular emission of a single molecule *Phys. Rev. Lett.* **85** 5312–5
[28] Lieb M A, Zavislan J M and Novotny L 2004 Single-molecule orientations determined by direct emission pattern imaging *J. Opt. Soc. Am.* B **21** 1210–5
[29] Taminiau T H, Stefani F D, Segerink F B and van Hulst N F 2008 Optical antennas direct single-molecule emission *Nat. Photonics* **2** 234–7